

X-ray Flares in Early GRB Afterglows

BY D. N. BURROWS¹, A. FALCONE¹, G. CHINCARINI^{2,3}, D. MORRIS¹, P. ROMANO², J. E. HILL^{4,5}, O. GODET⁶, A. MORETTI², H. KRIMM⁴, J. P. OSBORNE⁶, J. RACUSIN¹, V. MANGANO⁷, K. PAGE⁶, M. PERRI⁸, M. STROH¹,
AND THE *Swift* XRT TEAM

¹*Department of Astronomy & Astrophysics, The Pennsylvania State University, 525 Davey Lab, University Park, PA 16802, USA*

²*INAF-Osservatorio Astronomico di Brera, Via Bianchi 46, 23807 Merate, Italy*

³*Dipartimento di Fisica, Università degli studi di Milano-Bicocca, Piazza delle Scienze 3, 20126 Milano, Italy*

⁴*NASA/Goddard Space Flight Center, Greenbelt, MD 20771, USA*

⁵*Universities Space Research Association, 10211 Wincopin Circle, Suite 500, Columbia, MD, 21044-3432, USA*

⁶*Department of Physics & Astronomy, University of Leicester, Leicester LE1 7RH, UK*

⁷*INAF-Istituto di Astrofisica Spaziale e Fisica Cosmica, Sezione di Palermo, via U. La Malfa 153, I-90146 Palermo, Italy*

⁸*ASI Science Data Center, via G. Galilei, I-00044 Frascati, Italy*

The *Swift* X-ray Telescope (XRT) has discovered that flares are quite common in early X-ray afterglows of Gamma-Ray Bursts (GRBs), being observed in roughly 50% of afterglows with prompt followup observations. The flares range in fluence from a few percent to $\sim 100\%$ of the fluence of the prompt emission (the GRB). Repetitive flares are seen, with more than 4 successive flares detected by the XRT in some afterglows. The rise and fall times of the flares are typically considerable smaller than the time since the burst. These characteristics suggest that the flares are related to the prompt emission mechanism, but at lower photon energies. We conclude that the most likely cause of these flares is late-time activity of the GRB central engine.

Keywords: Gamma-ray Bursts; GRB Afterglows; X-ray Flares

1. Introduction

The advent of modern Gamma-Ray Burst (GRB) astronomy occurred in 1997 with the dramatic discovery by the *Beppo-SAX* satellite of the first GRB afterglow (Costa et al., 1997). This led to the identification of GRB host galaxies, the determination of their redshifts (and hence, their distances), and the measurement of important physical properties such as total energy. These observations provided strong evidence supporting the fireball model (Mészáros, 2002, and references therein), which attributes the burst itself and the subsequent afterglow to shocks generated by a highly relativistic fireball ejected from the GRB progenitor.

The typical *Beppo-SAX* afterglow observation began 6-8 hours after the burst (Frontera et al., 2000), and therefore early X-ray afterglows were only observed for a handful of cases before 2004. Piro et al. (2005) reported *Beppo-SAX* light

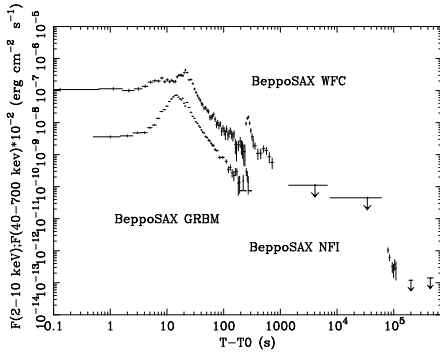


Figure 1. *Beppo-SAX* combined light curves of GRB 011121 (from Piro et al., 2005) from the Gamma-Ray Burst Monitor (GRBM), Wide Field Camera (WFC), and Narrow Field Instruments (NFI).

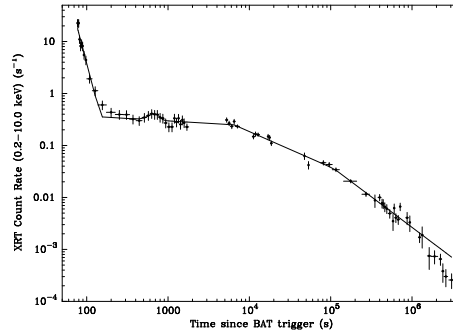


Figure 2. *Swift*/XRT light curve of GRB 060428A, which shows all of the phases seen in early GRB X-ray afterglows (but with an unusual dual-slope energy injection phase).

curves for two extremely bright bursts (GRB011121 and GRB011211) in which the early afterglow was captured by the Wide Field Camera before the satellite was re-pointed. Both of these early afterglows contained bright X-ray flares several hundred seconds after the burst, in which the flux increased rapidly by a factor of several (e.g., the flare peaking at ~ 270 s in figure 1). These events were attributed to the onset of the external shock in the circumburst medium. Such observations were quite rare until recently.

The *Swift* satellite (Gehrels et al., 2004) was specifically designed to study early GRB afterglows by automatically and immediately slewing to GRBs discovered on-board. The satellite carries three instruments: the wide-field Burst Alert Telescope (BAT: Barthelmy et al., 2005a), which detects bursts and provides a coarse position on the sky (typically < 3 arcminutes); and two narrow-field instruments: the X-ray Telescope (XRT: Burrows et al., 2005a) and the UV/Optical Telescope (UVOT: Roming et al., 2005). Prompt slews are successfully executed for $> 80\%$ of bursts detected by the BAT, and the afterglows are observed intensively by the XRT and UVOT for hours, days or weeks, depending on the burst. The XRT is designed to switch automatically between different readout modes in order to optimize the science as the afterglow fades (Hill et al., 2004). Because *Swift* is in a low Earth orbit (95 minute orbital period), there are gaps in the light curves when the satellite is on the wrong side of the Earth to view the burst.

In virtually every case, the XRT detects a fading X-ray afterglow of the burst. The resulting data set has provided the first comprehensive study of the early X-ray afterglows of GRBs in the time interval of ~ 0.1 to ~ 20 ks post-burst. We have found that the typical X-ray afterglow light curve follows a canonical template (Nousek et al., 2006; Zhang et al., 2006; O’Brien et al., 2006), well illustrated by the case of GRB 060428A (figure 2). This canonical light curve is a broken power law ($F_x \propto [t - T_0]^{-\alpha_x}$, where T_0 is the time at which the burst was detected) with flares superimposed. The first phase consists of a rapid decline in brightness from the burst itself (with $\alpha_x \sim 6$ in this case), which is attributed to light delay effects from the expanding shock (Kumar & Panaitescu, 2000). This is followed by a flat plateau phase (in this case, the plateau phase has two parts, with $\alpha_x \sim$

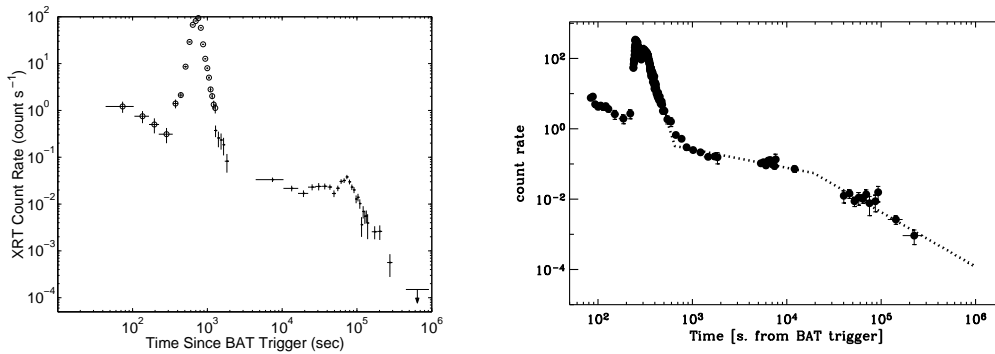


Figure 3. Giant X-ray flares. Left: X-ray light curve of GRB 050502B (0.2-10 keV), from Falcone et al. (2006). Open circles are Windowed Timing (WT) mode data and dots are Photon-Counting (PC) mode data (with pile-up corrections where necessary). Right: X-ray light curve of GRB 060526. Dotted lines show the underlying afterglow.

0.1 and 0.7), probably produced by energy injection into the external shock; a ‘normal’ afterglow with $\alpha_x \sim 1.3$, and sometimes a late break to $\alpha_x \sim 2.3$ when the edge of the collimated jet becomes visible. Detailed discussions of the physics behind these phases can be found in Nousek et al. (2006); Zhang et al. (2006), and Panaitescu et al. (2006). Although very few afterglows exhibit all of these phases, most afterglows can be characterized as a combination of at least two of them.

Roughly half of the afterglows have X-ray flares superimposed on this broken power-law light curve. The flare in GRB 060428A is fairly weak, peaking only $\sim 30\%$ in excess of the underlying power law level, but is otherwise typical of the flares observed with the XRT. We note that in this case, the flaring occurs during the plateau phase of the afterglow, that the afterglow from the external forward shock is already in progress when the flare begins, and that the light curve returns to this afterglow decay following the flare. Several examples of these flares have been discussed by Burrows et al. (2005b), Romano et al. (2006a), Falcone et al. (2006), and Pagani et al. (2006). Here we provide a more comprehensive look at the properties of these X-ray flares and what they can tell us about the GRB itself.

2. Case Studies

(a) Giant flares: GRBs 050502B and 060526

By way of contrast with the tiny flare of GRB 060428A, we next consider the giant flares seen in GRB 050502B and GRB 060526 (figure 3). GRB 050502B is discussed in detail by Falcone et al. (2006). The afterglow was initially faint, but the flux increased dramatically by a factor of ~ 500 , beginning about 345 s after the burst and peaking at about 700 s. The total X-ray fluence of the flare, 1×10^{-6} erg cm $^{-2}$ in the 0.2-10 keV band, is comparable to the 15-350 keV fluence of the gamma-ray burst itself. Like GRB 060428A, the flare appears to be superimposed on a power law decay that continues at the same slope after the flare ends; we will refer to this as the ‘underlying afterglow’ in subsequent discussion. The underlying afterglow in the case of GRB 050502B has a decay slope of $\alpha_x \sim 0.8$. The afterglow begins before the commencement of XRT observations (and before

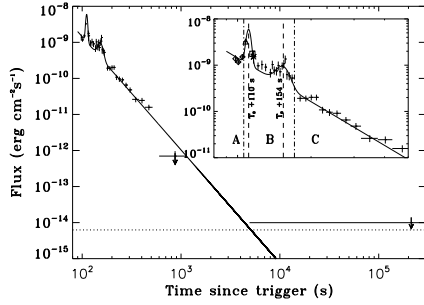


Figure 4. *Swift*/XRT 0.3-10 keV light curve of GRB 050421, a possible ‘naked’ GRB with a strong flare (Godet et al., 2006a).

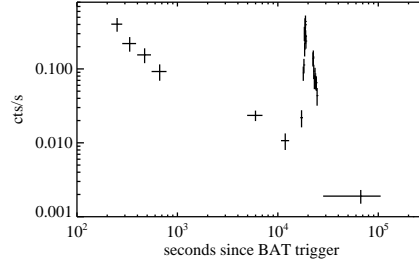


Figure 5. X-ray light curve of GRB 050916. A strong flare ($\sim 100\times$ the afterglow brightness) at about 20 ks is superimposed on an afterglow with decay index $\alpha_x \sim 1.5$.

the flare begins) and continues after the flare ends. The giant flare in GRB 060526 is remarkably similar, with a flux increase of about $100\times$ relative to the underlying afterglow, which also has $\alpha_x \sim 0.8$. In this case, the giant flare clearly consists of two separate, overlapping flares, peaking at about 220 s and 300 s. The level of the underlying afterglow before the flares is less clear than in GRB 050502B. Giant flares like these so dominate the light curve that they are reminiscent of the gamma-ray burst itself, although at lower energies and much longer time-scales. We will see that these two differences (energy range and time-scale) may be related.

(b) Flaring in a ‘naked’ GRB: GRB 050421

Figure 4 shows the X-ray light curve of GRB 050421 (Godet et al., 2006a). This light curve has a single power-law decay ($\alpha_x \sim 3.1$) with at least two flares superimposed, including the large (but poorly-sampled) flare at T_0+110 s. There is no hint in this light curve of any flattening due to the presence of an afterglow from the forward shock; in fact, there is no evidence for any interaction of the shock with the external medium. This GRB is therefore considered to be a possible ‘naked’ GRB, i.e., a GRB located in an extremely low density region (Kumar & Panaitescu, 2000). The absence of measured forward shock emission (to levels orders of magnitude below typical afterglow fluxes), combined with the presence of multiple flares in the light curve, therefore provides strong evidence that these flares originate elsewhere, perhaps in internal shocks within the relativistic outflow.

(c) Flares early and late

X-ray flares or bumps have been observed in all phases of the X-ray light curves, though they occur primarily in the first hour after the burst. For example, the flares in GRB 060607A occur during the initial steep decay, whilst those in GRB 050502B and GRB 060526 (figure 3), as well as GRB 060428A (figure 2), occur during the flat plateau. In a few cases we find a strong, rapidly rising and decaying flare at quite late times, such as the giant flare of GRB 050916 (figure 5). This is clearly similar to the early strong flares seen in other bursts.

GRB 050730 (figure 6) has a light curve that continues to flare at times as late as 35 ks post-burst. We attribute this variability to flaring, even though distinct flares

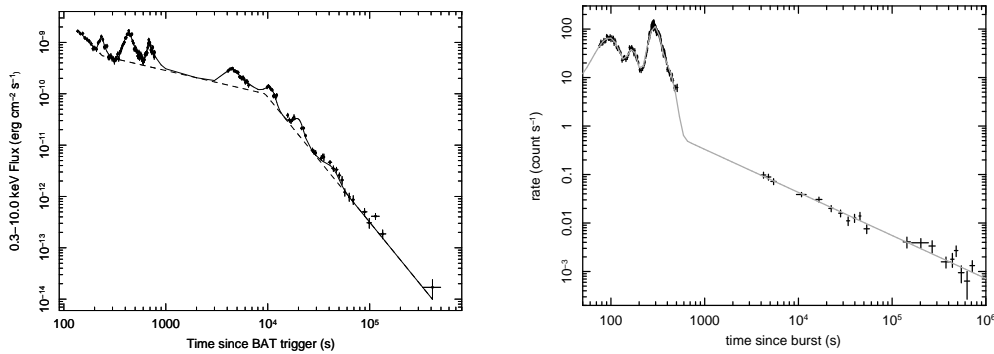


Figure 6. Left: X-ray light curve of GRB 050730 (0.3-10 keV) (Starling et al., 2005; Pandey et al., 2006). The dashed line indicates a possible underlying power-law decay, and the solid line indicates a possible fit to the decay curve with a set of flares. However, this light curve has so much variability that the level and slope of any underlying afterglow cannot be established with certainty. At least 3 strong flares are seen in the WT mode data of the first orbit. Right: X-ray light curve of GRB 060111A. Three strong flares are seen in the data from the first orbit.

are not visible in this case, because it is not possible to fit any simple series of power laws to this light curve. We note that a power law decay slope is established between 4.5 ks and 7 ks post-burst, and the light curve drops back to an extrapolation of this decay slope in the interval around 25 ks, consistent with intervening flares on top of an underlying afterglow. By contrast, other mechanisms for increased count rates, such as refreshed shocks, add energy into the external shock and thereafter the decay continues at a higher level instead of dropping back to the original curve.

(d) Flare multiplicity

In addition to isolated single flares, XRT light curves have many examples of multiple flares, such as those shown in figure 6. The light curves of GRB 050730 and GRB 060111A both begin with at least three X-ray flares of roughly equal peak flux (or count rate). This argues against single-shot flare mechanisms, such as the onset of the afterglow. (O’Brien et al., 2006, cite other evidence suggesting that the onset of the afterglow occurs very early in the light curve, probably prior to the rapid decline phase at the end of the last gamma-ray pulse.)

(e) X-rays from GRB peaks

Figure 7 shows the BAT and XRT light curves for GRB 060306. In this burst, the BAT detected three distinct peaks of activity, with the last occurring at about T_0+44 s. By the time the XRT began observations at T_0+100 s the prompt activity had ended, and the XRT observations begin with the steep decay of the tail of the prompt emission.

Had the XRT observations of GRB 060306 started before T_0+40 s, both XRT and BAT would have observed the third peak of the prompt emission. In fact, this has happened for a number of long-lasting bursts, including GRB 050117 (Hill et al., 2006), GRB 050713A (Morris et al., 2006), GRB 050820A (Cenko et al., 2006), GRB 060124

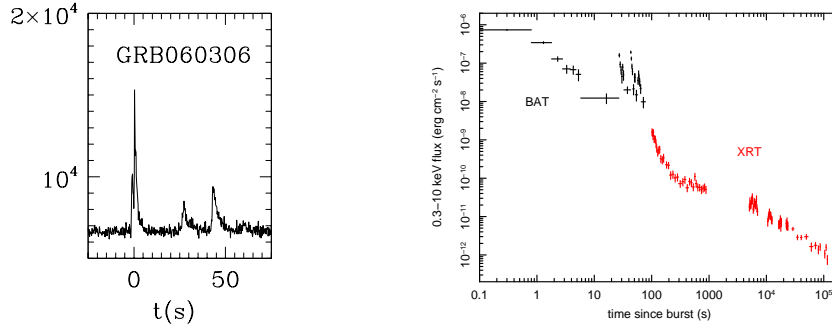


Figure 7. Left: *Swift*/BAT light curve of GRB 060306. The BAT measures three distinct peaks in the burst light curve, spread out over about 44 s. Right: Combined light curve of the BAT (extrapolated into the XRT energy band) and XRT observations of GRB 060306. No flares are seen in the XRT light curve, which begins with the tail of the last BAT peak.

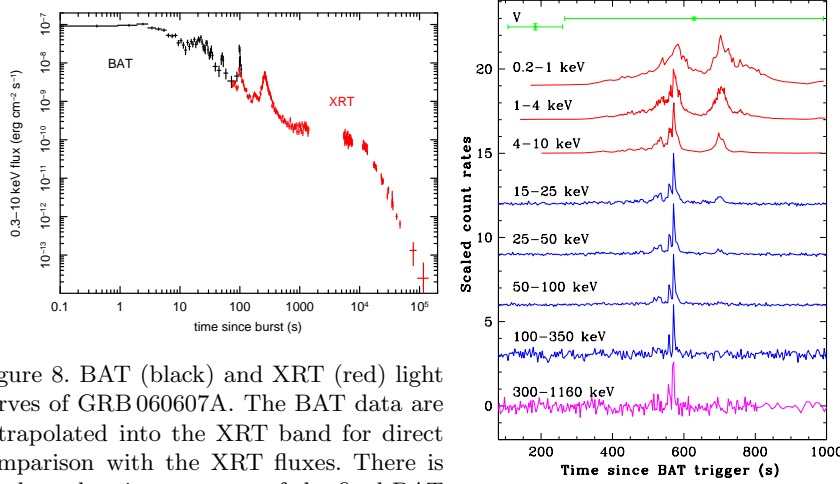


Figure 8. BAT (black) and XRT (red) light curves of GRB 060607A. The BAT data are extrapolated into the XRT band for direct comparison with the XRT fluxes. There is good overlapping coverage of the final BAT peak at about T_0+100 s, with the XRT detecting several later, fainter flares. Note that the XRT peak at 100 s is much broader than the corresponding BAT peak, and that the broader soft X-ray profile is very similar to that of the later X-ray flares.

Figure 9. Light curves of the main burst of GRB 060124 (from Romano et al., 2006b) as measured by (from top to bottom): the *Swift* UVOT (V band), XRT (0.2–10 keV), and BAT (15–350 keV), and by Konus-Wind (300–1160 keV).

(Romano et al., 2006b), GRB 060418, GRB 060510B, GRB 060607A, and GRB 060714. In figure 8 we show a recent example. The BAT and XRT observed this burst in the 15–150 keV and 0.2–10 keV bands, respectively. Spectral evolution is evident in the different relative strengths and widths of the peaks as detected by the two instruments. In general, the soft X-ray manifestations of the prompt peaks are significantly broader than the peaks observed in the hard X-ray band, as is clear from the light curves of GRB 060607A, in which it is also clear that the soft X-ray peak is very similar to the later X-ray flares. The energy dependence of the prompt peaks is particularly evident in GRB 060124 (Romano et al., 2006b), which was detected by

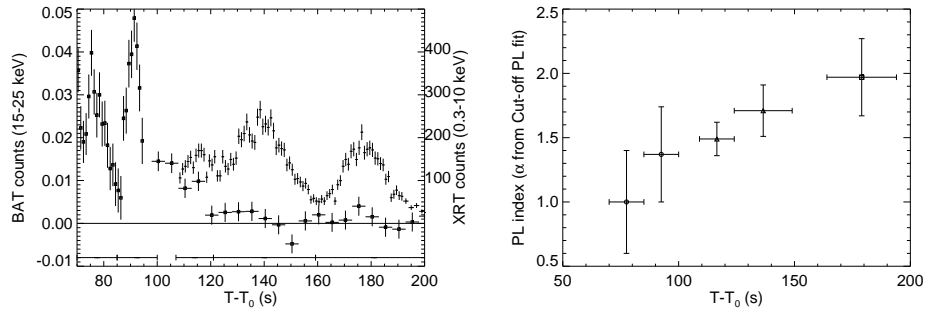


Figure 10. Left: BAT (boxes) and XRT (crosses) light curves for GRB 060714. The horizontal bars indicate the time periods used in the spectral fits of the individual BAT and XRT peaks. Right: Photon index for a power law spectral model with exponential cut-off at high energies for five peaks in the BAT/XRT light curve of GRB 060714. The first two peaks were fit to only the BAT data, the third peak was fit to XRT and BAT data simultaneously, and the last two peaks were fit to only the XRT data.

both *Swift* and *Konus-Wind* and so has very broad-band coverage. Figure 9 shows the main burst of GRB 060124 as a function of energy from the optical (V band) to γ -ray (1 MeV). This burst had a particularly long period of activity, with a precursor that triggered the BAT nearly 10 minutes before the main burst. This later pulse is very narrow at high energies, but is quite broad in the soft X-ray band, and is followed by a very similar, but much softer X-ray flare that is barely detected by the BAT above 15 keV. The only distinction between this later X-ray flare and the earlier gamma-ray burst appears to be the spectral distribution of the photons. We note that this event would have been classified as an X-Ray Flash (XRF) had it consisted only of this later flare.

(f) Spectral evolution during flares

These giant flares are so bright that detailed spectral analysis is possible. Detailed spectral analysis for GRB 050502B is discussed in Falcone et al. (2006), who also showed that a simple hardness ratio shows strong spectral evolution, increasing steeply at the beginning of the flare, peaking well before the flare itself peaks, and then dropping gradually through the remainder of the flare, finally returning to the same level established in the afterglow emission before the flare. This behaviour is also seen in other bursts with sufficient statistics: e.g., GRBs 050607 (Pagani et al., 2006), 050822 (Godet et al., 2006a), 051117A, and 060607A (Chincarini, 2006). This spectral evolution results from a hard-to-soft transition in the X-ray flare similar to that commonly seen in GRB prompt emission (e.g., Ford et al., 1995; Frontera et al., 2000; Piro et al., 2005).

A particularly interesting example is GRB 060714, in which a series of pulses in the BAT energy range (15-350 keV) is followed by a similar series in the XRT band (0.2-10 keV). The spectra of these pulses can be fit with a cut-off power law model, giving clear evidence of spectral evolution (figure 10), with the spectrum becoming successively softer with each new peak.

Similar behavior is observed in a number of other flares, and includes apparent transitions of the emission from the gamma-ray or hard X-ray bands into the soft X-ray band as time progresses. For example, observationally we see in both

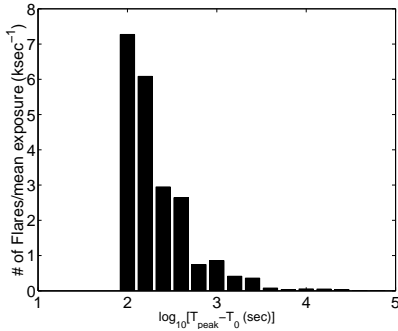


Figure 11. Distribution of peak times of X-ray flares in our sample, normalized to the exposure time in each bin.

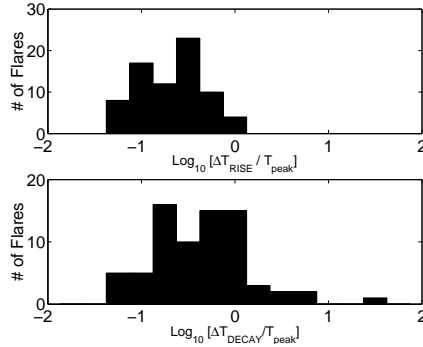


Figure 12. Distributions of rise and decay times for flares in our sample.

GRB 060714 and GRB 060418 that the final, weak BAT pulse is seen in the XRT as a strong flare. This transition to softer pulses can be clearly seen in GRB 060124 (figure 9). As a final example, our analysis of GRB 050416A finds evidence that E_{peak} moves from the BAT band into the XRT band (Mangano et al., 2006). This suggests a strong connection between the X-ray flares and the prompt emission - they appear to be the same phenomenon, simply expressed at lower energies at later times.

(g) *Flares in short GRB afterglows: GRBs 050724 and 051210*

So far we have only discussed flares in long GRBs, which are thought to be the result of the collapse of massive stars into black holes. Two short GRBs, GRB 050724 (Barthelmy et al., 2005b; Campana et al., 2006; Grupe et al., 2006) and GRB 051210 (La Parola et al., 2006), also have flares in their X-ray light curves. This requires that short GRB models, which typically invoke mergers of compact objects (two neutron stars or a neutron star and a black hole), must also be capable of producing flares. Of particular interest in this regard is the very late and energetic event at about 12 hours post-burst in GRB 050724, a very late time-scale for a merger process thought to last only milliseconds.

3. Statistical analysis

Having examined some ‘case studies’ illustrative of the properties of the X-ray flares, we now turn to a more objective statistical treatment of their properties. We are undertaking a comprehensive study of the properties of flares using a set of 77 flares in 33 XRT afterglows. Here we simply highlight a few preliminary results related to the temporal properties of X-ray flares in GRB afterglows.

The distribution of peak times of flares is shown in figure 11. The times are in the observer frame, uncorrected for redshift (since we do not have redshifts for many of these bursts). The distribution follows a power law with slope of -1.1, with flares strongly concentrated at early times. This is not surprising if the X-ray flares represent the last sputters of the GRB, but further work must be done to determine whether this distribution can be used to rule out other models for the flares.

An important clue to the nature of the flares can be found by analysing their rise and decay times. Mechanisms such as external shocks encountering clouds in the circumburst medium are expected to produce rather slow rise and decay times, with decay times characterized by $\Delta t/t \sim 1$ (Ioka et al., 2005; Nakar & Granot, 2006). By contrast, the pulses associated with collisions of shocks within the relativistic outflow (‘internal shocks’) are typically much faster, with $\Delta t/t \ll 1$. The X-ray flares span both ranges, with some having $\Delta t/t \sim 0.1$ or less. For example, figure 5 shows a case of a narrow, late flare.

In order to ascertain the rise and decay times, we have fit each flare in our sample of 77 flares with a model consisting of an underlying power law decay with a flare superimposed on it. We fit both the rising portion of the flare and its decay with power laws. We then define Δt_{rise} as $t_p - t_1$, where t_p is the peak time (the time when the rising power law intersects the decaying power law), and t_1 is the time when the rising power law intersects the underlying afterglow’s power law decay. Similarly, the decay time is defined as $\Delta t_{decay} = t_2 - t_p$, where t_2 is the time when the falling power law tail of the flare crosses the underlying power law decay. Figure 12 shows the distributions of rise and decay times for our sample. The distributions peak near $\Delta t/t \sim 0.3$, uncomfortably short for external shocks.

4. Discussion

X-ray flares in GRB afterglows could be produced by a variety of mechanisms, including internal shocks (the same mechanism that produces the GRB prompt emission) at late times, external forward shocks (either the onset of the forward shock or encounters by the forward shock of density gradients or clouds), or external reverse shocks. Based on the observations described above, we believe that there is strong evidence that X-ray flares in early GRB afterglows are not produced by the external shock (forward or reverse). This view is supported by: 1) the rapid rise and decay times of most X-ray flares; 2) the multiplicity of many X-ray flares, which cannot be explained by ‘single-shot’ mechanisms like the onset of the afterglow; 3) the fact that some flares are clearly superimposed on a pre-existing afterglow decay; 4) the observation of flares in ‘naked’ afterglows with no evidence for forward shock emission (e.g., GRB 050421); 5) the enormous increase in flux in giant flares.

By contrast, all of these characteristics are easily accommodated by internal shocks. Internal shocks can also explain the following observational characteristics of X-ray flares: 1) the similarity between the shapes of X-ray flares and X-ray peaks in the prompt emission; 2) the spectral evolution of X-ray flares, both within individual flares and between successive flares, which mimics that commonly seen in the prompt emission. Additional support for the view that X-ray flares are due to internal shocks comes from the analysis of Liang et al. (2006), who showed that the decay slopes of X-ray flares are consistent with the expectations of the ‘curvature effect’ (time delay effects from an extended shock front following the cessation of the emission; Kumar & Panaitescu, 2000) We conclude that X-ray flares in GRB afterglows are probably the result of late-time internal shocks.

These late internal shocks can be produced in at least two ways. In the internal shock model (Rees & Mészáros, 1994), the central engine activity produces a series of shells of outflowing material with a variety of Lorentz factors, and the GRB prompt emission results from ‘internal shocks’ as these shells collide in the

relativistic outflow. Such collisions can occur over a wide range of timescales, with late shocks resulting from collisions between shells with Lorentz factors that differ by only a small amount. These could produce X-ray flares at relatively late times. The fact that these late-time collisions must occur at large radii may lead to a natural explanation for the relatively soft photon emission. On the other hand, this mechanism may not be able to produce the required efficiency of conversion of kinetic energy of the jet to afterglow flux, due to the weakness of the resulting shock (Zhang, 2006).

A second possibility is that the late internal shocks are the result of continued activity in the central engine itself. In this case, the central engine must remain active for time-scales up to ten times longer than the prompt emission, with important implications for GRB models. For long GRBs, the leading collapsar model would need to explain in-fall of material into the central black hole over time-scales of hours. For short GRBs, a similar problem exists in the context of merging compact objects. We note that the redshift of the GRB can play a role in delaying flaring activity in the observer's frame, and also in broadening the flares. This cannot be the sole explanation for late, broad X-ray flares, however; even in the case of GRB 050904, with redshift $z = 6.29$, flaring occurs for over an hour in the burst rest frame (Watson et al., 2006; Cusumano et al., 2006). Furthermore, the mean redshift of flaring GRBs ($z = 2.6$ for 14 flaring GRBs with known redshifts) does not differ significantly from those without flares, so the X-ray flares are not simply due to prompt emission delayed, broadened, and reduced in peak energy by high redshifts. We conclude that the central engines of GRBs remain active for hours following the GRB event.

This work is supported at Penn State by NASA contract NAS5-00136, at OAB by ASI grant I/R/039/04, and at the University of Leicester by funding from PPARC.

References

- Barthelmy, S. D., et al. 2005a The Burst Alert Telescope (BAT) on the SWIFT Midex Mission. *Space Sci. Rev.*, **120**, 143-164.
- Barthelmy, S. D., et al. 2005b An origin for short γ -ray bursts unassociated with current star formation. *Nature*, **438**, 994-996.
- Burrows, D. N., et al. 2005a The Swift X-Ray Telescope. *Space Sci. Rev.*, **120**, 165-195.
- Burrows, D. N. et al. 2005b Bright X-ray Flares in Gamma-Ray Burst Afterglows. *Science*, **309**, 1833-1835.
- Campana, S., et al. 2006 The X-ray afterglow of the short gamma ray burst 050724. *Astr. & Ap.*, **454**, 113-117.
- Cenko, S. B., et al. 2006, *Ap. J.*, in press, *astro-ph/0608183*.
- Chincarini, G. 2006 GRBs with the Swift satellite. In *Proc. of Vulcano Workshop 2006, Frontier Objects in Astrophysics and Particle Physics* (ed. F. Giovannelli & G. Mannocchi), in press. Bologna:Italian Physical Society, Editrice Compositori, *astro-ph/0608414*.

- Costa, E., et al. 1997 Discovery of an X-ray afterglow associated with the gamma-ray burst of 28 February 1997. *Nature*, **387**, 783-785.
- Cusumano, G., et al. 2006 Gamma-ray bursts: Huge explosion in the early Universe. *Nature*, **440**, 164.
- Falcone, A., et al. 2006 The Giant X-Ray Flare of GRB 050502B: Evidence for Late-Time Internal Engine Activity. *Ap. J.*, **641**, 1010-1017.
- Ford, L. A., et al. 1995 BATSE observations of gamma-ray burst spectra. 2: Peak energy evolution in bright, long bursts. *Ap. J.*, **439**, 307-321.
- Frontera, F., et al. 2000 Prompt and Delayed Emission Properties of Gamma-Ray Bursts Observed with BeppoSAX. *Ap. J. Suppl.*, **127**, 59-78
- Gehrels, N., et al. 2004 The Swift Gamma-Ray Burst Mission. *Ap. J.*, **611**, 1005-1020.
- Godet, O., et al. 2006a X-ray flares in the early Swift observations of the possible naked gamma-ray burst 050421. *Astr. & Ap.*, **452**, 819-825.
- Godet, O., et al. 2006b Swift XRF 050822: Internal processes versus cocoon breakout. *Astr. & Ap.*, submitted.
- Grupe, D., Burrows, D. N., Patel, S. K., Kouveliotou, C., Zhang, B., Mészáros, P., Wijers, R. A. M., & Gehrels, N. 2006 Jet breaks in Short Gamma-ray Bursts. I: The Uncollimated Afterglow of GRB 050724. *Ap. J.*, in press, *astro-ph/0603773*.
- Hill, J.E., et al. 2004 Readout modes and automated operation of the Swift X-ray Telescope. *Proc. SPIE*, **5165**, 217-231.
- Hill, J.E., et al. 2006 GRB 050117: Simultaneous Gamma-Ray and X-Ray Observations with the Swift Satellite. *Ap. J.*, **639**, 303-310.
- Ioka, K., Kobayashi, S., & Zhang, B. 2005 Variabilities of Gamma-Ray Burst Afterglows: Long-acting Engine, Anisotropic Jet, or Many Fluctuating Regions? *Ap. J.*, **631**, 429-434.
- Kumar, P., & Panaitescu, A. 2000 Afterglow Emission from Naked Gamma-Ray Bursts. *Ap. J.*, 541, L51-L54.
- La Parola, V., et al. 2006 GRB 051210: Swift detection of a short gamma ray burst. *Astr. & Ap.*, **454**, 753-757.
- Liang, E., et al. 2006 Testing the Curvature Effect and Internal Origin of Gamma-Ray Burst Prompt Emissions and X-Ray Flares with Swift Data. *Ap. J.*, **646**, 351-357.
- Mangano, V., et al. 2006 Swift XRT Observations of the Afterglow of XRF 050416A. *Ap. J.*, in press, *astro-ph/0603738*.
- Mészáros, P. 2002 Theories of Gamma-Ray Bursts. *ARA&A*, **40**, 137

- Morris, D. C., et al. 2006 GRB 050713A: High Energy Observations of the GRB Prompt and Afterglow Emission. *Ap. J.*, in press, *astro-ph/0602490*
- Nakar, E., & Granot, J. 2006 Smooth Light Curves from a Bumpy Ride: Relativistic BlastWave Encounters a Density Jump. *MNRAS*, submitted, *astro-ph/0606011*
- Nousek, J. A., et al. 2006 Evidence for a Canonical Gamma-Ray Burst Afterglow Light Curve in the Swift XRT Data. *Ap. J.*, **642**, 389-400.
- O'Brien, P. T., et al. 2006 The Early X-Ray Emission from GRBs. *Ap. J.*, **647**, 1213-1237.
- Pagani, C., et al. 2006 The Swift X-Ray Flaring Afterglow of GRB 050607. *Ap. J.*, **645**, 1315-1322.
- Panaitescu, A., Mészáros, P., Gehrels, N., Burrows, D., & Nousek, J. 2006 Analysis of the X-ray emission of nine Swift afterglows. *MNRAS*, **366**, 1357-1366.
- Pandey, S. B., et al. 2006 Multi-wavelength afterglow observations of the high redshift GRB 050730. *Astr. & Ap.*, in press, *astro-ph/0607471*.
- Piro, L., et al. 2005 Probing the environment in Gamma-ray bursts: the case of an X-ray precursor, afterglow late onset and wind vs constant density profile in GRB 011121 and GRB 011211. *Ap. J.*, **623**, 314-324.
- Rees, M. J., & Mészáros, P. 1994 Unsteady outflow models for cosmological gamma-ray bursts. *Ap. J.*, **430**, L93-L96.
- Romano, P. et al. 2006a X-ray flare in XRF 050406: evidence for prolonged engine activity. *Astr. & Ap.*, **450**, 59-68.
- Romano, P., et al. 2006b Panchromatic study of GRB 060124: from precursor to afterglow. *Astr. & Ap.*, **456**, 917-927.
- Roming, P.W.A., et al., 2005 The Swift Ultra-Violet/Optical Telescope. *Space Sci. Rev.*, **120**, 95-142.
- Starling, R.L.C., et al. 2005 Gas and dust properties in the afterglow spectra of GRB 050730. *Astr. & Ap.*, **442**, L21-L24.
- Watson, D., Reeves, J. N., Hjorth, J., Fynbo, J. P. U., Jakobsson, P., Pedersen, K., Sollerman, J., Castro Cerón, J. M., McBreen, S., Foley, S. 2006 Outshining the Quasars at Reionization: The X-Ray Spectrum and Light Curve of the Redshift 6.29 Gamma-Ray Burst GRB 050904. *Ap. J.*, **637**, L69-L72.
- Zhang, B., Fan, Y.Z., Dyks, J., Kobayashi, S., Mészáros, P., Burrows, B.N., Nousek, J.A., & Gehrels, N., 2006 Physical Processes Shaping Gamma-Ray Burst X-Ray Afterglow Light Curves: Theoretical Implications from the Swift X-Ray Telescope Observations. *Ap. J.*, **642**, 354-370.
- Zhang, B., 2006 Gamma-Ray Burst Afterglows. *Advances in Space Research*, submitted.

